Constructing of Bi_2WO_6 with double active sites of tunable metallic Bi and oxygen vacancy for photocatalytic oxidation of cyclohexane to cyclohexanone

Jun-Lei Wang,[a] Kuan Wang,[*a] Zhen-Hong He,[a] Tong Sun,[a] Run-Jing You[a], Jian-Gang Chen,[b] Weitao Wang,[a] Yang Yang,[a] Zhao-Tie Liu[*a,b]

[a]Key Laboratory of Chemical Additives for China National Light Industry, College of Chemistry and Chemical Engineering, Shaanxi University of Science and Technology, Xi'an, 710021, China

[b]School of Chemistry & Chemical Engineering, Shaanxi Normal University, Xi'an, 710119, China

Corresponding Author

*E-mail: wangkuan@sust.edu.cn (K. Wang), ztliu@snnu.edu.cn (Z.-T. Liu).

The possible mechanisms of the OV-Bi/Bi_2WO_6 for the photothermal oxidation of cyclohexane are summarized as follows.

$$Bi_2WO_6 + h\nu \rightarrow Bi_2WO_6\ (h^+ + e^-) \quad (1)$$

$$O_2 + e^- \rightarrow \cdot O_2^- \quad (2)$$

$$\cdot O_2^- + 2H^+ + e^- \rightarrow H_2O_2 \rightarrow 2\cdot OH \quad (3)$$

$$C_6H_{12} + h^+ \rightarrow C_6H_{11}\cdot + H^+ \quad (4)$$

$$C_6H_{11}\cdot + O_2 \rightarrow C_6H_{11}OO\cdot \quad (5)$$

$$2C_6H_{11}OO\cdot \rightarrow C_6H_{10}O + C_6H_{11}OH + O_2 \quad (6)$$

$$C_6H_{11}OO\cdot + e^- + H^+ \rightarrow C_6H_{10}O + H_2O \quad (7)$$

$$C_6H_{11}OH + 2h^+ \rightarrow C_6H_{10}O + 2H^+ \quad (8)$$

$$C_6H_{11}OH + 2\cdot OH \rightarrow C_6H_{11}O + 2H_2O \quad (9)$$

$$C_6H_{11}\cdot + \cdot O_2^- \rightarrow C_6H_{11}O + OH^- \quad (10)$$

$$C_6H_{12} + O_2 \rightarrow C_6H_{11}OOH \quad (11)$$

$$C_6H_{11}OOH \rightarrow C_6H_{11}O\cdot + \cdot OH \quad (12)$$

$$C_6H_{11}O\cdot + C_6H_{12} \rightarrow C_6H_{11}OH + C_6H_{11}\cdot \quad (13)$$

$$C_6H_{12} + \cdot OH \rightarrow C_6H_{11}\cdot + H_2O \quad (14)$$

$$C_6H_{11}\cdot + O_2 \rightarrow C_6H_{11}OO\cdot \quad (15)$$

$$C_6H_{11}\cdot + \cdot OH \rightarrow C_6H_{11}OH \quad (16)$$

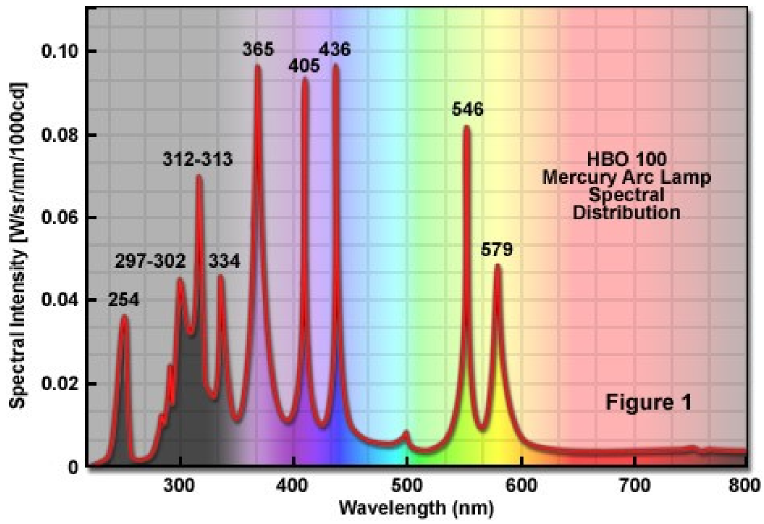

Fig. S1. The wavelength image of the Hg lamp

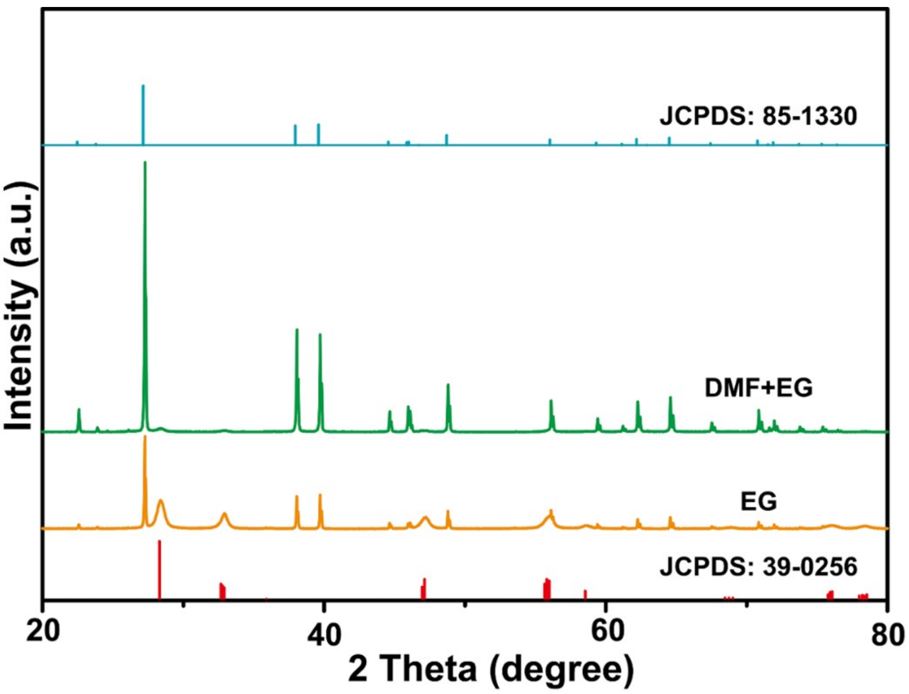

Fig. S2. XRD patterns of OV-Bi/Bi_2WO_6 in EG and EG+DMF

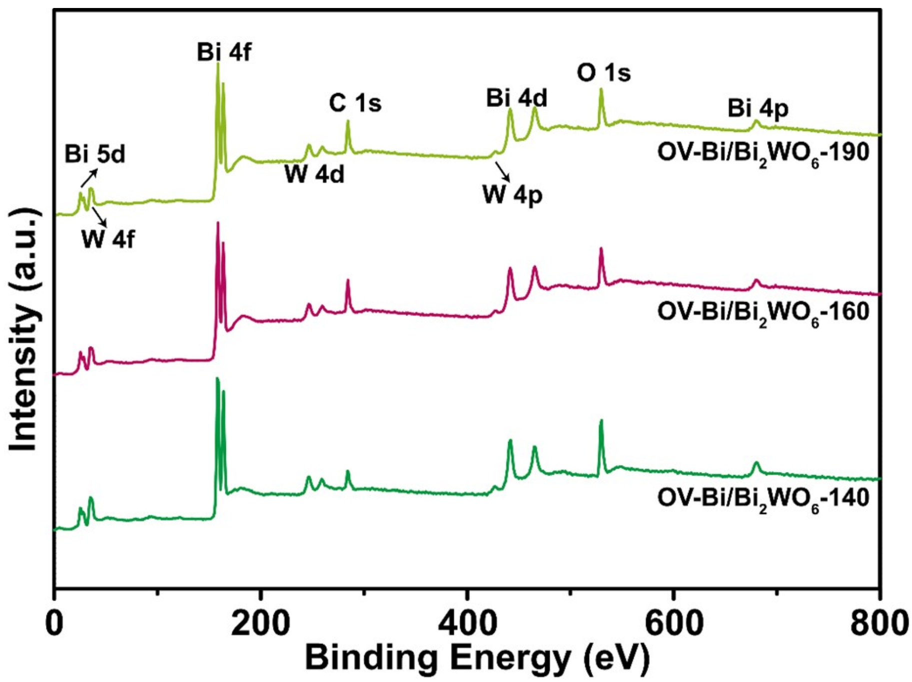

Fig. S3. The survey spectrum of OV-Bi/Bi_2WO_6-140, OV-Bi/Bi_2WO_6-160, and OV-Bi/Bi_2WO_6-190.

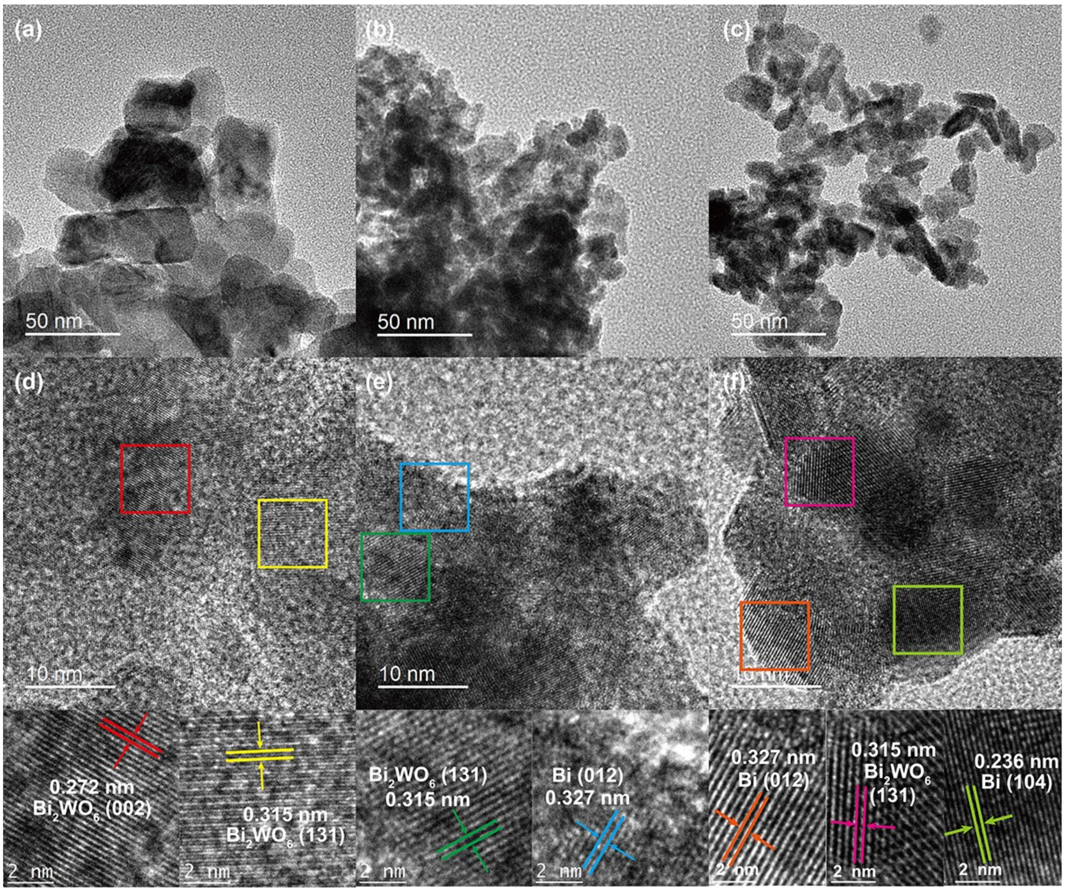

Fig. S4. TEM and HRTEM of (a, d) OV-Bi/Bi_2WO_6-150, (b, e) OV-Bi/Bi_2WO_6-170, (c, f,) OV-Bi/Bi_2WO_6-180.

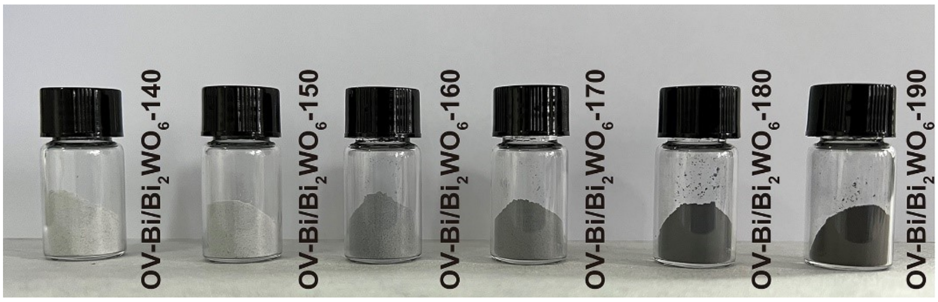

Fig. S5. The color of OV-Bi/Bi_2WO_6

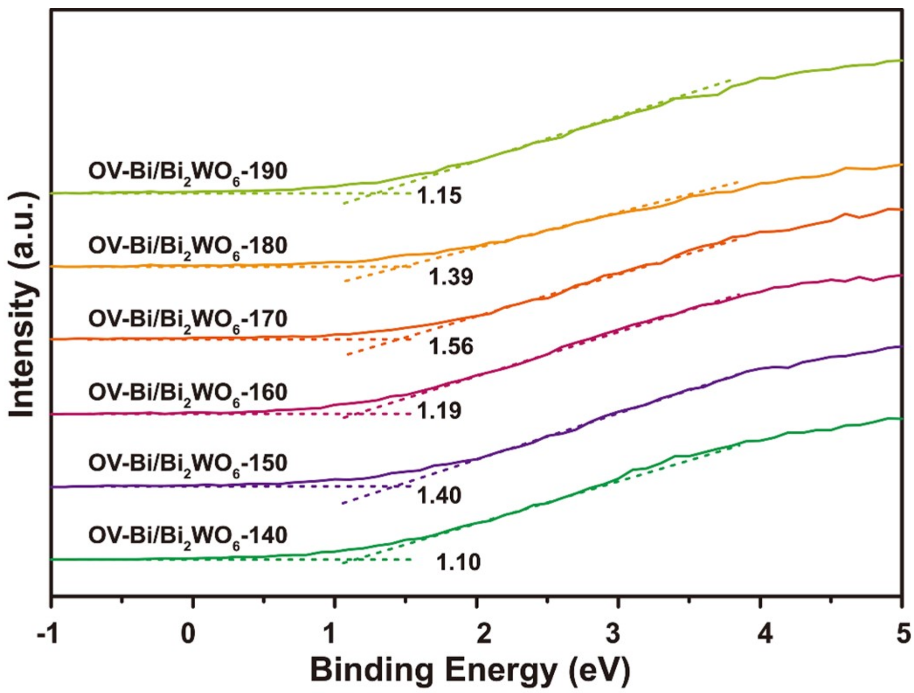

Fig. S6. VB-XPS spectra of samples of OV-Bi/Bi_2WO_6

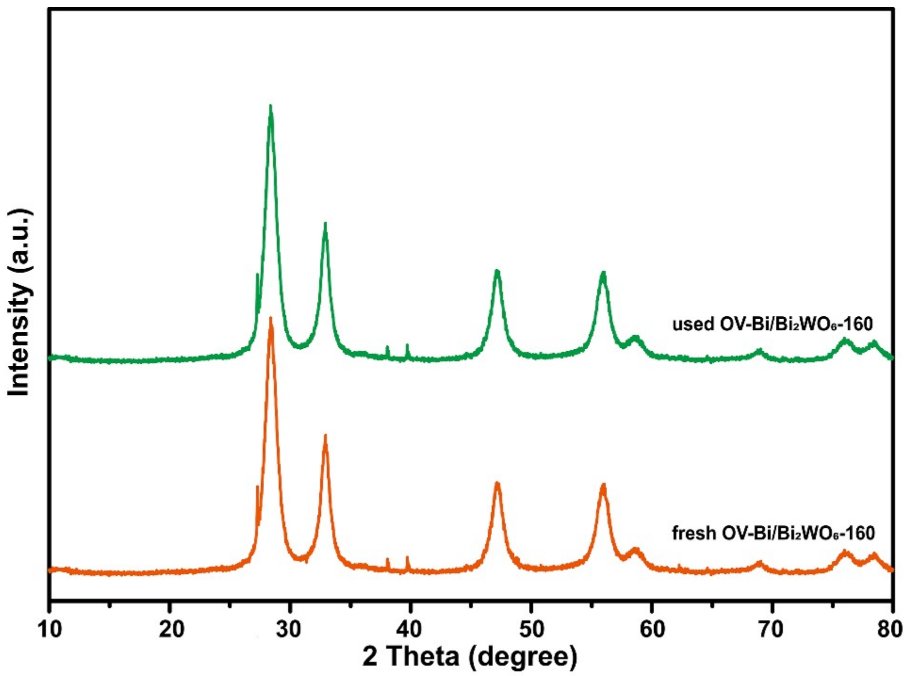

Fig. S7. XRD patterns of used and fresh OV-Bi/Bi_2WO_6-160 sample.

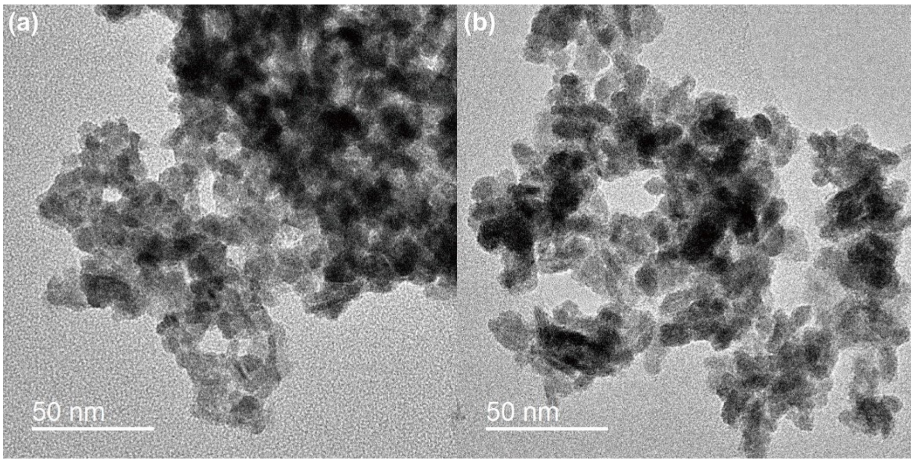

Fig. S8. TEM images of used and fresh OV-Bi/Bi_2WO_6-160 sample.

Table S1 Photocatalytic activities comparison of reported for the photocatalytic oxidation of CHA

Catalysts	Reaction condition	Oxidant	CHA-one		Ref.
			Amounts/μmol	Sel./%	
TiO_2/rGO$_{0.5}$	20 mg cat., 5 mL CHA, 2000 W Xe Lamp (λ>300 nm), 12 h	1 atm O_2	40.1	83.0	[S1]
h-BN/TiO_2	50 mg cat., 3 mL CHA, 300 W Xe Lamp (λ>300 nm), 12 h	1 atm O_2	43.9	85.4	[S2]
In_2O_3/N-TiO_2	50 mg cat., 3 mL CHA, 300 W Xe Lamp (λ>300 nm), 12 h	1 atm O_2	46.3	89.7	[S3]
N-TiO_2-3	50 mg cat., 10 mL CHA, 10 mL CCl_4, 300 W Xe Lamp (λ>420 nm), 5 h	0.1 MPa O_2	112.4	100	[S4]
AFO/SBA	30 mg cat., 1.5 mL CHA, 18.5 mL CAN, solar simulator, 24 h	1 atm O_2	70	51	[S5]
$BiVO_4$	50 mg cat., 4 mM CHA, 5 mL CAN, 20 W W-Br lamp, 8 h	1 atm O_2	72.6	72.6	[S6]
BiOI-10	25 mg cat., 24.975 mL CHA, 0.025 mL H_2O, 400 W metal halides-lamp, 3 h	1 atm air	3.1	98.75	[S7]
BiOI	25 mg cat., 24.975 mL CHA, 0.025 mL H_2O, 400 W metal halides-lamp, 3 h	1 atm air	20.2	99.3	[S8]
OV-BiOCl-P	50 mg cat., 3 mL CHA, 500 W Hg lamp, 10 h	1 atm air	228.1	81.1	[S9]
OV-Bi/BiOCl-160	50 mg cat., 3 mL CHA, 500 W Hg lamp, 10 h	1 atm air	128.9	93.6	This work

Table S2 Fluorescence emission lifetime and relevant percentage data fitted by a bi-exponential function

Samples	τ_1 (ns)	A_1 (%)	τ_2 (ns)	A_2 (%)	τ_a (ns)
OV-Bi/Bi_2WO_6-140	0.7407	75.24	5.0545	24.76	3.73
OV-Bi/Bi_2WO_6-160	0.8569	59.76	4.7606	40.24	3.94
OV-Bi/Bi_2WO_6-190	0.9918	92.34	5.5807	7.66	2.45

The decay curves could be well-fitted by a biexponential function:

$$I_{(t)} = I_0 + A_1\exp(-t/\tau_1) + A_2\exp(-t/\tau_2) \quad (1)$$

where A_1 and A_2 represent the excited state emission decay amplitudes, I_0 is a constant about the baseline offset, τ_1 refers to the fast decay of trap-mediated nonradiative recombination, and τ_2 is the slow decay correlated to radiative recombination [S10,S11].

The average lifetime is calculated from the following equation:

$$\tau_a = (A_1\tau_1^2 + A_2\tau_2^2) / (A_1\tau_1 + A_2\tau_2) \quad (2)$$

References

[S1]. Y. Shiraishi, S. Shiota, H. Hirakawa, S. Tanaka, S. Ichikawa, T. Hirai, Titanium dioxide/reduced graphene oxide hybrid photocatalysts for efficient and selective partial oxidation of cyclohexane, ACS Catal. 7 (2017) 293-300.

[S2]. K. Wang, B. Xue, J. Wang, Z. He, X. Zhang, S. Li, W. Wang, Y. Yang, Z. Liu, Efficient and selective oxidation of cyclohexane to cyclohexanone over flake hexagonal boron nitride/titanium dioxide hybrid photocatalysts, Mol. Catal. 505 (2021) 111530.

[S3]. K. Wang, B. Xue, J.Wang, Z.-H. He, S.-S. Li, D.Wang, W.-T. Wang, Y. Yang, and Z.-T. Liu, Construction of Indium Oxide/N-Doped Titanium Dioxide Hybrid Photocatalysts for Efficient and Selective Oxidation of Cyclohexane to Cyclohexanone, J Phys. Chem. C, 125(36) (2021) 19791-19801.

[S4]. G. Xu, Y. Zhang, D. Peng, D. Sheng, Y. Tian, D. Ma, Y. Zhang, Nitrogen-doped mixed-phase TiO_2 with controllable phase junction as superior visible-light photocatalyst for selective oxidation of cyclohexane, Appl. Surf. Sci. 536 (2021) 147953.

[S5]. Y. Ide, S. Tominaka, Y. Yoneno, K. Komaguchi, T. Takei, H. Nishida, N. Tsunoji, A. Machida, T. Sano, Condensed ferric dimers for green photocatalytic synthesis of nylon precursors, Chem. Sci. 10 (2019) 6604-6611.

[S6]. L. Xiang, J. Fan, W. Zhong, L. Mao, K. You, D. Yin, Heteroatom-induced band-reconstruction of metal vanadates for photocatalytic cyclohexane oxidation towards KA-oil selectivity, Appl. Catal. A Gen. 575 (2019) 120-131.

[S7]. D. Contreras, V. Melin, K. Márquez, G. Pérez-González, H. Mansilla, G. Pecchi, A. Henríquez, Selective oxidation of cyclohexane to cyclohexanol by bioi under visible light: Role of the ratio (110)/(001) facet, Appl. Catal. B Environ. 251 (2019) 17-24.

[S8]. A. Henríquez, H. Mansilla, A. Martínez-de la Cruz, J. Freer, D. Contreras, Selective oxofunctionalization of cyclohexane over titanium dioxide-based and bismuth oxyhalide (BiOX, X=Cl^-, Br^-, I^-) photocatalysts by visible light irradiation, Appl. Catal. B Environ. 206 (2017) 252-262.

[S9]. J. Wang, K. Wang, Z.-H. He, R.-R. Zhang, P. Guo, W. Wang, Y. Yang, Z.-T. Liu, Constructing of ultrathin Bi_2WO_6/BiOCl nanosheets with oxygen vacancies for photocatalytic oxidation of cyclohexane with air in solvent-free, Appl. Surf. Sci. 584 (2022): 152606.

[S10] S. Meng, C. Chen, X. Gu, H. Wu, Q. Meng, J. Zhang, S. Chen, X. Fu, D. Liu, W. Lei, Efficient photocatalytic H_2 evolution, CO_2 reduction and N_2 fixation coupled with organic synthesis by cocatalyst and vacancies engineering, Appl. Catal. B Environ. 285 (2021) 119789.

[S11] Y. Yang, Z. Zeng, G. Zeng, D. Huang, R. Xiao, C. Zhang, C. Zhou, W. Xiong, W. Wang, M. Cheng, W. Xue, H. Guo, X. Tang and D. He, Ti_3C_2 mxene/porous g-C_3N_4 interfacial Schottky junction for boosting spatial charge separation in photocatalytic H_2O_2 production, Appl. Catal. B Environ. 258 (2019) 117956.